HHS Public Access

Author manuscript

Epilepsia. Author manuscript; available in PMC 2019 January 01.

Published in final edited form as:

Epilepsia. 2018 January ; 59(1): 123–134. doi:10.1111/epi.13942.

Hepatic and hippocampal Cyp enzymes over-expression during spontaneous recurrent seizures

Leonie Runtz[1,*], **Benoit Girard**[2,*], **Marion Toussenot**[1], **Julie Espallergues**[4], **Alexis Fayd'Herbe De Maudave**[1], **Alexandre Milman**[6], **Frederic deBock**[1], **Chaitali Ghosh**[3], **Nathalie C. Guérineau**[6], **Jean-Marc Pascussi**[5], **Federica Bertaso**[2], and **Nicola Marchi**[1]

[1]Laboratory of Cerebrovascular Mechanisms of Brain Disorders, Institute of Functional Genomics (UMR 5203 CNRS – U 1191 INSERM), Montpellier, France

[2]Laboratory of Pathophysiology of Synaptic Transmission, Institute of Functional Genomics (UMR 5203 CNRS – U 1191 INSERM), Montpellier, France

[3]Cerebrovascular Research, Cleveland Clinic, USA

[4]Histalim, Montpellier, France

[5]Laboratory of self-renewal and differentiation of epithelia, Institute of Functional Genomics (UMR 5203 CNRS – U 1191 INSERM), Montpellier, France

[6]Ion channels in Neuronal Excitability and Diseases, Institute of Functional Genomics (UMR 5203 CNRS – U 1191 INSERM), Montpellier, France

Abstract

Objective—Available evidence points to a role of cytochrome P450 (Cyp) drug biotransformation enzymes in central nervous system (CNS) diseases, including epilepsy. Deviations in drug pharmacokinetic profiles may impact therapeutic outcomes. Here, we ask whether spontaneous recurrent seizure (SRS) activity is sufficient to modulate the expression of major Cyp enzymes in the liver and brain.

Methods—Unilateral intra-hippocampal (i.h) kainic acid (KA) injections were used to elicit non convulsive status epilepticus (SE), epileptogenesis, and spontaneous recurrent seizures (SRS), as monitored by video-electroencephalography. Intra-peritoneal (i.p) KA injection was used to trigger generalized tonic-clonic SE. KA injected mice and sham controls were sacrificed at 24–72 hours and 1 week post-SE (i.h or i.p KA), and during the chronic stage (SRS; 6 weeks post-i.h KA). Liver and brain tissues were processed for histology, RT-qPCR, western blot, or microsomal enzymatic assay. Cyp2e1, Cyp3a13, GFAP/IBA1, xenobiotic nuclear receptors nr1I2 (PXR), nr1I3

Corresponding Author: Dr. Nicola Marchi. Cerebrovascular Mechanisms of Brain Disorders, Institut de Génomique Fonctionnelle, CNRS UMR5203, INSERM U1191, Université Montpellier, 141 rue de la Cardonille, 34094 Montpellier, Cedex 5, France. nicola.marchi@igf.cnrs.fr.

*Equally contributed to this work

MR. BENOIT J GIRARD (Orcid ID : 0000-0002-3914-6483)

Disclosure of Conflicts of Interest. None of the authors has any conflict of interest to disclose.

Ethical Publication Statement. We confirm that we have read the Journal's position on issues involved in ethical publication and affirm that this report is consistent with those guidelines.

(CAR) and glucocorticoid (nr3c1; GR) expression was examined. Serum samples were obtained to assay corticosterone, a glucocorticosteroid receptor activator.

Results—A significant increase of Cyp3a13 and Cyp2e1 transcripts and protein expression was found in the liver and hippocampi during SRS, as compared to control mice. In the ipsilateral hippocampus, Cyp2e1 and Cyp3a protein upregulation during SRS positively correlated to GFAP expression. $GFAP^+$, and not $IBA1^+$, cells co-localized with Cyp2e1 or Cyp3a expression. In the liver, a trend increase in Cyp3a microsomal activity was found during SRS as compared to control mice. The transcript levels of the Cyp upstream regulators GR, xenobiotic nr1I2, and nr1I3 receptors were unchanged at SRS. Corticosterone levels, a GR ligand, were increased in the blood post-SE and during SRS.

Significance—SRS modifies Cyp expression in the liver and the hippocampus. Nuclear receptors or inflammatory pathways are candidate mechanisms of Cyp regulation during seizures.

Keywords

P450; liver; brain; epilepsy; drug metabolism

INTRODUCTION

The concept of a bidirectional brain-periphery interplay occurring during physiological and pathological states is emerging. Experimental and clinical evidence supports a role of peripheral pathologies in favoring the onset or the progression of central nervous system (CNS) diseases [1–3]. However, less is known on whether CNS diseases may impact peripheral organs' function. A number of players exist to potentially sustain a crosstalk during pathological conditions, including inflammatory signals, stress hormones, and cerebrovascular or neuronal routes [4–7].

Abnormalities in pharmacokinetic mechanisms in epilepsy have been previously outlined [8, 9]. Recently, cytochrome metabolic enzymes (Cyp) in the brain were suggested to possibly impact the biotransformation of xenobiotics or endogenous molecules in human epileptic subjects [10–15], a concept that transverses to several CNS pathologies [14, 16–21]. However, the role of spontaneous seizure activity and status epilepticus (SE) on brain Cyp expression remains to be clarified. Furthermore the possibility that, during spontaneous seizures, changes in Cyp expression may occur in the liver, a primary drug metabolic site in the periphery, has never been investigated. This latter hypothesis fits the concept of a brain-peripheral crosstalk, exporting pathophysiological signals beyond the brain's borders. This proposition could have a significant consequence by allowing pharmacokinetic aspects of drug regimens during CNS disease to be better defined or predicted. Previous studies in the epilepsy field have focused on peripheral aspects of disease, e.g., blood biomarkers, but have neglected direct effects on peripheral organs [7].

In the present study, we asked whether spontaneous recurrent seizures and SE in mice are associated with hepatic and brain Cyp expression changes. We evaluated two experimental models to elicit SE (non-convulsive and tonic-clonic) and spontaneous recurrent seizure (SRS), investigating changes in Cyp expression in the brain and liver. We focused on

Cyp2e1 and Cyp3a as their human homologues are responsible for the metabolism of a large array of anti-epileptic medications [14, 20, 22]. In addition, we evaluated the existence of pathophysiological modifications previously suggested to impact Cyp expression, namely astrocytosis [20] and nuclear receptor [23–27] – glucocorticosterone levels.

METHODS

Vertebrate animals

All experiments were performed according to the European Union (Council directive 86/609EEC) and institutional/local guidelines of laboratory animals' usage. Mice (male C57BL/6j, 8–10 weeks) were housed on a 12h light/dark cycle with food and water *ad libitum*. Animal protocols were approved by the French ethical committee for animal testing (05185.01; 0846.01 to NM and #8564 to FB). All efforts were directed at minimizing animal discomfort and to reduce the number of animals used (3R rule).

Kainic acid injection protocols, video-EEG monitoring and signal analysis

We used two experimental models to: i) elicit convulsive (intra-peritoneal kainic acid) or non-convulsive (intra-hippocampal kainic acid) status epilepticus (SE); ii) generate a steady yield of spontaneously seizing mice (intra-hippocampal kainic acid).

Intra-hippocampal kainic acid injection [28–31]—Mice were anesthetized with chloral hydrate and placed in a stereotaxic frame. A 10μL micro-syringe (stainless steel 33G needle) was filled with a 20 mM solution of kainic acid (KA; Sigma-Aldrich) in 0.9% sterile NaCl, and positioned in the right dorsal hippocampus (AP = −2, ML = −1.5, DV = −2 mm). Mice were injected (over a 1 minute) with 50 nL of KA solution (1 nmol), using a micro-pump operating the micro-syringe. After injection, the cannula was left in place for an additional 2 min to avoid reflux. Sham mice were injected with 50 nL of 0.9% sterile NaCl. Mice were implanted with a bipolar electrode in correspondence of the injection site. Mice were also equipped with three monopolar electrodes placed on the right fronto-parietal cortex, while the reference was placed on the cerebellum (cortical EEG traces *not shown*). Electrodes were secured on the skull using dental acrylic cement. After surgery the animals were kept under observation for 8h to assess the behavioral changes corresponding to SE [28–30]. Generally, i.h KA elicited non-convulsive SE, with mild asymmetric clonic movements of the forelimbs along with deviations of the head, rotations, and periods of stillness [31]. In some cases, bilateral clonic seizures associated with rearing were observed [30, 31]. Video-EEG recording was performed using a Pinnacle Technology wired system (Lawrence, KS, USA). Signals acquisition (Sirenia®, Pinnacle Technology Inc.) was filtered at 40 Hz, and sampling set at 200–400 Hz. Video was synchronized to the EEG. Mice were monitored daily starting from 1 week post-SE and for the 5 consecutive weeks (at least 3 hours/session) to detect spontaneous recurrent seizure (SRS). The occurrence of SRS activity was characterized using EEG analysis (pClamp, Sirenia) and criteria derived from previously published guidelines [28–30]. Briefly: i) rhythmic sharp waves were selected when their amplitude was > 2 × baseline; ii) spike activity of > 5 sec duration was considered a seizure; iii) two distinct seizures were separated by > 1 sec one from another. Figure 2 provides quantifications of seizure activity and the number of seizures calculated according to the

above criteria and normalized by EEG recording time (hour). Scoring in Figure 2H–H1 is proportional to the duration of the longest hippocampal discharges detected for each mouse during 3 consecutive EEG sessions performed between weeks 1 and 5. The latter method was previously described by [29] and it reflects the level of maturation of an epileptic network and epileptogenesis.

Intra-peritoneal kainic acid injection—Mice were anesthetized using ketamine/xylazine and placed in a stereotaxic frame. Intra-hippocampal bipolar electrodes were implanted (AP = −2.5, ML = −3.4, DV = −2.7). See above for surgery details. Behavior was scored according to the Racine scale during SE as induced by i.p. kainic acid injection (KA, 25 mg/kg; stock solution 5 mg/ml KA in PBS, pH = 7 adjusted with NaOH 0.2M). Animals were selected when a generalized tonic-clonic SE associated with a loss of balance was observed (Stage VI Racine). We chose animals experiencing at least 3 tonic-clonic convulsive SE (lasting at least 30–45 seconds over a period of 90 min).

The following groups of animals were generated using intra-hippocampal kainic acid injections: sham control, 24h–72h, 1 week (n= 5–6 / group) and 6 weeks post-KA (n = 9). Two separate series of animals were used to perform histology, western blots and RT-qPCR (PFA fixed vs. snap frozen), leading to a total of n = 20–24 × 2 mice (up to 1 week) and 9 × 2 mice (6 weeks). Intra-peritoneal kainic acid injections were also performed to obtain: sham control, 24h–72h, 1 week (n= 5–6 mice / group). Two series: n= 20–24 × 2 mice. Samples obtained from 24h and 72h groups were pulled together to increase the number of animals. Mice were processed as follows: i) intracardiac perfusion with 4% PFA + overnight post-fixation for brain and liver histology. Livers were transferred to 30% EtOH; ii) intracardiac perfusion with PBS and liver and hippocampi were snap frozen for western blot and RT-qPCR analysis; iii) blood samples were obtained from the left cardiac ventricles prior to PBS/PFA perfusions. Models efficiency: i) i.h KA non-convulsive SE induction rate 100%, mortality 2 out of 52 (~4%) occurring during SE; ii) i.p KA convulsive SE induction rate 75%, mortality 9 out 34 (~25%) during SE or 24 hours after.

Real-time quantitative PCR

Total cellular RNA was isolated and genomic DNA contamination was removed using the RNeasy Mini RNA isolation kit (*Qiagen*). 2 μg of total RNA was reverse-transcribed using random hexamers and the MMLV reverse transcriptase kit (Invitrogen). Real-time quantitative PCR was performed in a LightCycler 480 apparatus (*Roche Diagnostic, Meylan, France*) with a SYBR green based detection assay (Roche). Reactions were conducted in a 10-μl volume of 50 ng cDNA, 300 nM of each primer, and 5 μl of SYBR Green PCR Master Mix at 95 C for 10 min, 40 cycles of denaturation at 95°C for 10 s, annealing at 61°C for 20 s, elongation at 72°C for 20 s. Amplification specificity was confirmed for each sample by determining the melting curve. The levels of cDNA were quantified by the comparative threshold cycle method using β-actin and/or gapdh as an internal standard. Primers are listed in Supplemental Table 1. Supplemental Figure 1B shows examples of reporter genes (Ct) determined in 3 separate experiments using all samples (CTR to SRS), confirming consistency and stability of the read-outs.

Western Blots

Liver samples were homogenized in buffer (500 μl) containing: 0.1% SDS, protease inhibitor cocktail (Promega), 50 mM Tris-HCL (pH 7.4), 10 mM EDTA, 1 mM Na3VO4, 40 mM sodium pyrophosphate, 50 mM NaF, and 1 mM DTT. After centrifugation (12,000 rpm for 10 min), samples were separated by electrophoresis and then transferred onto a nitrocellulose membrane (Lifescience). After 1 hour of blocking the membranes were probed 4°C (overnight) with a rabbit monoclonal Cyp2e1 (1:1000, Abcam ab151544) or rabbit polyclonal to human Cyp3A4 also recognizing mouse Cyp3a (1:2000, Abcam ab176310) and a mouse anti-Actin (1:10000, Abcam ab6276). Goat anti-rabbit (1:4000, Jackson Immuno, 111-035-003) and goat anti-mouse HRP conjugated (1:4000, Jackson Immuno, 115-035-003) antibodies were used for Cyp2e1, Cyp3a or b-actin. Immunoreactivity was detected with an enhanced chemiluminescence method (ECLTM plus detection reagent, GE Healthcare) and signals were quantified using ImageJ.

Microsomal fraction isolation and enzyme activity assay

Microsome preparations were obtained from hepatic tissues using the Biovision Microsome Isolation Kit (product #K249). Mice (n = 9 SRS and n = 6 control) were perfused intracardially with PBS, the livers dissected and homogenized using the reagents provided by the vendor. After centrifugation, the microsomal pellets were suspended in storage buffer and kept at −80°C. Protein concentration was determined using a Thermo Scientific NanoDrop 2000 (absorbance at 280nm). Cyp3a4 activity was quantified using a Promega™ P450-Glo assay (#V9001). Briefly, microsomal fractions (96-well plate) were combined with a selective substrate (Luciferin-IPA) for 10 min at 37°C. The enzymatic reaction was initiated using a NADPH regenerating system supplied by the vendor. A luciferin detection reagent was added and the luminescent signal quantified (Lifesciences Tecan Infinite 200; integration time of 1000ms/well). The standard curve was determined using D-Luciferin (0.016, 0.08, 0.4, 2 and 10 μM).

Corticosterone measurement

Blood samples were collected from the left cardiac ventricle using heparinized needle/containers and centrifuged (425g, 10 minutes at 4C). For each sample, the serum was separated and stored at −80C. Quantitative determination of corticosterone was performed using a colorimetric competitive enzyme immunoassay (Corticosterone EIA kit, Enzo Cat n° ADI-900-097) according to the vendor protocol.

Brain and liver immunohistochemistry

All liver samples were processed for dehydration / paraffin embedding using a Peloris automaton (Leica). Briefly, 4 μm paraffin sections were stained using a Discovery XT automaton (Ventana - Roche) and the ChromoMap DAB detection kit (Roche-Ventana; 05266645001). Tris/EDTA pH8–8.5 antigen retrieval was performed and Cyp immunoreactivity was detected using the following rabbit polyclonal antibodies: anti-Cyp2E1 (1:50; Abcam; ab28146) or anti-Cyp3A4 (1:200; Abcam; ab176310). After 1 hour of incubation (37°C) samples were treated (16 min at 37°C) with an OmniMap anti-rabbit antibody (Roche-Ventana; 05269679001). Liver sections were counterstained with

hematoxylin (Hematoxylin II, 05277965001; Bluing reagent, 05266769001; Roche-Ventana). Slides were dehydrated and cover-slipped with DPX mounting media. Images were acquired using a Nanozoomer scanner (Hamamatsu) in bright field condition (20x). Quantification of Cyp2E1 and Cyp3A signals was performed on randomly chosen whole liver slices. A Fiji semi-automatic routine was used to calculate pixel area normalized by total slice area x100.

Brain coronal sections were collected and washed three times with PBS. Sections were blocked using PBS containing 0.25% triton, and 20% normal horse serum (1h, room temperature). Slices were incubated overnight at 4°C with primary antibody (PBS containing 0.1% triton): Cyp2E1 (polyclonal rabbit, 1:200, Abcam, Ab28146), Cyp3A4 (polyclonal rabbit, 1:100, Abcam, Ab176310), GFAP (polyclonal chicken, 1:1000, Abcam, Ab4674), IBA1 (polyclonal rabbit, 1:2000, Wako, 019-19741). After 3 washes, secondary antibodies were incubated 2 hours (room temperature). Cyp2E1 and Cyp3A immunoreactivity was imaged using a fluorescent microscope (Apotome Z-stacks 20x and 40x; montage 10x; Zeiss, AxioImager Z1).

Statistics

Data were analyzed using parametric or non-parametric (Mann-Whitney) tests depending on normality distribution (Shapiro-Wilcox). Student's *t*-test with equal variances was used for groups of 2, when relevant. Linear plots were analyzed using a Pearson (r values) correlation analyses. In all cases, significance was < 0.05. Statistical analyses were performed using GraphPad Prism 6.0 (GraphPad Prism Software Inc., San Diego, USA) or Origin Microcal.

RESULTS

Hippocampal and hepatic Cyp over-expression during spontaneous recurrent seizures

We asked whether brain Cyp expression was modified during spontaneous recurrent seizures (SRS), as elicited by unilateral intra-hippocampal KA injection[30]. Hippocampal Cyp2E1 and Cyp3a13 transcripts were significantly increased in SRS mice as compared to control (Figure 1A1–A2). Cyp3a13 is a gene isoform coding for the Cyp3A protein in mice [21]. Cyp and GFAP transcript increase was significant in the ipsilateral as compared to the contralateral hippocampi, where Cyp transcripts did not change (Supplemental Figure 1A–A2). A positive correlation was found between GFAP immunoreactivity and Cyp transcript levels (Figure 1B–B1). Cyp3a11 isoform transcripts were significantly lower (RT-qPCR Ct > 33) than Cyp3A13 and did not change between experimental groups (*not shown*). Montages in Figure 1C–C1 depict the typical brain topography of GFAP hippocampal immunoreactivity occurring during SRS. Cyp2e1 expression was increased at SRS (ipsilateral>contralateral; Figure 1D–D1), co-localizing with GFAP (Figure 1F). Cyp3a expression was increased at SRS (Figure 1G). Z-plane reconstructions indicate an example of Cyp2e1 expression at the end-feet glial-microvascular interface (Figure 1H). Although causality is not implied, these results indicate GFAP immunoreactivity concomitant to hippocampal Cyp over-expression during spontaneous recurrent seizures.

The hepatic levels of Cyp2e1 and Cyp3a13 transcripts (Figure 2A–A1) and proteins (CYP2e1 and Cyp3a, Figure 2B–B1) were subsequentially evaluated. A significant increase in Cyp expression was found during SRS in the liver. Figure 2C–D shows examples of Cyp2e1 and Cyp3a immunohistochemistry performed on hepatic tissues obtained from control and SRS mice. Hepatic Cyp3a11 transcripts were detected, although they did not change (*data not shown*). Abundance of Cyp mRNA levels in the liver as compared to the hippocampi was confirmed as an internal control (Supplemental Figure 1C–C1). Examples of intra-hippocampal EEG traces recorded 1 week after i.h. KA and during SRS are shown in Figure 2E–E1 and F, color-coded to examples of scoring plots (Figure 2G–G1). Hepatic Cyp2E1 and Cyp3a expression positively correlated with SRS scores (Figure 2H–H2; see Methods for details). An initial evaluation of Cyp metabolism was then performed. Hepatic microsomal fractions were extracted to quantify enzymatic activity. We found a trend increase in Cyp3a4 activity during SRS (mean ± sem: 141.67 ± 7.51 pmol D-Luciferin/mg microsomal fraction protein/min) as compared to control mice (mean ± sem: 80.45 ± 30.63; $p = 0.08$). In this experiment SRS mice experience an average of 33.2 ± 4.3 seizures/h. In summary, these results indicate Cyp up-regulation in the liver during spontaneous recurrent seizures.

Status Epilepticus dysregulates hippocampal and hepatic Cyp expression

We examined whether Cyp expression was impacted early after SE (convulsive or not [30, 31]). Hippocampal Cyp expression was qualitatively evaluated up to 1 week after i.h. or i.p. KA injections (Figure 3). The combination of the two models allows overcoming confounding factors such as: i) direct KA hepatic/brain tissue effects unrelated to seizures; ii) tissue lesions due to cannula/electrodes insertion. IBA1 and GFAP activation was confirmed (Figure 3A). We found an incremental Cyp2e1 and Cyp3A astrocytic expression consequent to either i.h. (Figure 3C) or i.p. (Figure 3D–E) KA induced SE. Z-stack reconstructions confirmed $GFAP^+$ astrocyte Cyp2e1 and Cyp3a colocalization, while neuronal expression of Cyp3a was also observed (*arrrows* in Figure 3E). $IBA1^+$ microglial activation did not colocalize with Cyp expression. Table 1 summarizes RT-qPCR data.

The effect of SE on hepatic Cyp levels was also investigated. No significant changes or a transient decrease in Cyp2e1 or Cyp3a13 transcripts were found 24–72 hours post-SE (i.h and i.p KA; Table 1). Figure 4A–B shows modulation of Cyp proteins occurring 24–72 hours after convulsive SE (i.p KA). In particular, a qualitatively decreased Cyp3a and increased Cyp2e1 protein expression was detected after SE in the liver. Supplemental Figure 1D–D3 provides box plot examples of Cyp transcript and protein levels in the i.h. KA model. These results suggest short-term and differential patterns of hepatic Cyp modulation depending on SE.

Serum corticosterone and hepatic nuclear receptor levels

In peripheral organs, the expression of Cyp enzymes is directly controlled by upstream xenobiotic (NR1i) and glucocorticoid (GR) nuclear receptors [26, 27]. The latter is activated by endogenous ligands, *e.g.,* cortisol in humans and corticosterone in mice [32]. Interestingly, clinical evidence indicates a post-ictal cortisol increase in the blood of epileptic patients [33–35]. We therefore performed an initial analysis of nuclear receptors expression and

corticosterone levels following SE or during SRS in mice. The hepatic expression of GR and NR1i transcripts was stable throughout disease progression (Figure 5A–C). Figure 5D depicts changes in serum corticosterone occurring after SE as induced by i.p. or i.h. KA injections. Mean corticosterone level was increased during SRS, although a significant variability existed between mice. We are aware that corticosterone half-life is short and that the exact interval between the last SRS and blood collection could not be accounted for. We speculate that hepatic Cyp over-expression during SRS may result from corticosterone fluctuations activating specific nuclear receptors in the liver.

DISCUSSION

The results presented indicate the up-regulation of specific Cyp in the liver and hippocampi during SRS. Cyp2e1 and Cyp3a13 (Cyp3a protein) expression changes in response to seizures could affect both peripheral and CNS drug biotransformation routes. This study was designed to elucidate whether a chronic disease is sufficient to modify the expression of biotransformation enzymes in the periphery in the absence of confounding factors, e.g., drugs targeting seizures and co-morbidities. Thus, it is recognized that cytochrome enzymes expression or activity can be induced by xenobiotics [21]. While human brain specimens can be available from surgical procedures performed to relieve drug resistant seizures, access to the patient's peripheral organs (e.g., liver) is improbable. The use of experimental models of seizures circumvents the latter problem.

Cyp expression and brain pathology

Accumulating evidence indicates the expression of numerous Cyp in brain cells, with results varying and depending on the species and sample preparation methods [10–12, 14, 36]. The original report of Cyp expression at peri-ventricular brain structures [12] was followed by evidence for Cyp and NR expression in isolated microcapillaries and in isolated brain primary cells or tissues [10, 14, 36]. Our results focus on Cyp2e1 and Cyp3a as they are implicated in the Phase 1 metabolism of numerous anti-epileptic drugs [14, 22] and modified in drug resistant epileptic human brain tissues [14]. Our results link GFAP immunoreactivity to brain Cyp over-expression during SRS. GFAP mRNA increase during SRS was less prominent in the contralateral as compared to the ipsilateral hippocampi (i.h. KA) and not associated to significant Cyp changes (Supplemental Figure 1A3–A4). Our results align with the pathophysiological significance of Cyp enzymes in CNS diseases, including Parkinson's disease, alcohol or drug dependence, and neurodegenerative diseases [16–20]. Although expressed at lower levels in the brain as compared to the liver, neuro-glio-vascular cytochromes are localized in the immediate proximity of neuronal drug targets, possibly representing a second line of xenobiotic biotransformation, with a potential impact on CNS drug efficacy or neurotoxicology.

Astrocyte Cyp over-expression is consistent with drug biotransformation occurring at the cerebrovascular interface (e.g., end-feet) and in the parenchyma. Our results also confirm Cyp expression in neurons, specifically Cyp3a. The latter fits evidence previously described in humans and rodents [37]. However, reports dealing with functional correlates of brain Cyp modulation *in vivo* are uncommon. Direct brain inhibition of specific Cyp or NR supported a

link between PXR or Cyp3a activity, neurosteroids metabolism, and cognitive or behavioral dysfunction [38, 39]. On the other hand, our initial results indicate a trend increase of Cyp3a metabolism in hepatic microsomes obtained from SRS mice, as compared to control. Additional studies are required to fully define the role of Cyp in metabolizing anti-epileptic drugs during epileptogenesis and SRS, in the liver and brain. Targeting Cyp enzymes or their upstream regulators nuclear receptors may have a clinical benefit.

Peripheral-CNS interplay in health and disease

A cause and effect between peripheral diseases and CNS pathologies is clinically recognized. For instance, metabolic disorders, diabetes or sustained peripheral inflammation can determine neurological symptoms, including psychiatric illnesses and seizures. In this case, cerebrovascular permeability is evoked as one of the participating culprits [7, 40]. The opposite route, *e.g.,* brain-driven peripheral changes, remains relatively understudied. The activation of vagal nerve or sympathetic and parasympathetic pathways in response to seizures has been proposed in epilepsy [41]. Our results support further studies to determine whether stress molecules (corticosterone, epinephrine, norepinephrine, etc.) released post-SE or during SRS can activate nuclear receptors in peripheral organs, resulting in Cyp expression changes. Thus, GR and NR1i2–PXR directly regulate Cyp3a transcription [26, 27, 32]. This hypothesis is supported by the clinical evidence of increased cortisol levels corresponding to ictal events in epileptic subjects[33–35]. We speculate that the hypothalamus-pituitary-adrenal (HPA) axis could also be involved, possibly explaining the fluctuation of stress hormones in blood. The latter remains to be investigated.

Pitfalls and Conclusions

We are aware that a number of caveats exist in the presented study. In particular: i) a lack of a comprehensive functional assays evaluating Cyp metabolism of AED during epileptogenesis and SRS; ii) the temporal correlation between SRS and corticosterone levels was not investigated; iii) the mechanism of corticosterone changes, e.g. HPA axis and adrenal cortex activation was only speculated; iv) corticosterone entry in the CNS and its effect was not evaluated; v) other peripheral organs of drug biotransformation (e.g. intestine) were not studied. The latter exceed the capacity of our current study but could be evaluated as a continuation of this research.

In conclusion, our results indicate that hepatic and brain players of drug biotransformation are modified during SRS. The existence of a mechanistic link between the peripheral and brain changes remains to be defined. The functional significance of Cyp regulation in epilepsy is important as we could improve drug efficacy and predict side effects. Nuclear receptors or inflammatory pathways may contribute to the changes in hepatic and brain Cyp expression during seizures and are therefore two potential targets to consider.

Supplementary Material

Refer to Web version on PubMed Central for supplementary material.

Acknowledgments

Support comes from NIH-NINDS R01 (NM/CG) and FFRE-FR1 (NM). We would like to thank Dr. Badreddine Boussadia for the initial discussion of the experimental plan. We would like to thank Dr. Antoine DePaulis for sharing his know-how on experimental models of seizures and Dr. Laurent Givalois for sharing expertise inherent to stress hormone biology and monitoring.

References

1. Bechmann I, Galea I, Perry VH. What is the blood-brain barrier (not)? Trends Immunol. 2007; 28:5–11. [PubMed: 17140851]
2. Chesnokova V, Pechnick RN, Wawrowsky K. Chronic peripheral inflammation, hippocampal neurogenesis, and behavior. Brain Behav Immun. 2016; 58:1–8. [PubMed: 26802985]
3. Roelofs K, Pasman J. Stress, childhood trauma, and cognitive functions in functional neurologic disorders. Handb Clin Neurol. 2016; 139:139–55. [PubMed: 27719835]
4. Bonaz BL, Bernstein CN. Brain-gut interactions in inflammatory bowel disease. Gastroenterology. 2013; 144:36–49. [PubMed: 23063970]
5. Chida Y, Sudo N, Kubo C. Does stress exacerbate liver diseases? J Gastroenterol Hepatol. 2006; 21:202–8. [PubMed: 16460474]
6. Tsigos C, Chrousos GP. Hypothalamic-pituitary-adrenal axis, neuroendocrine factors and stress. J Psychosom Res. 2002; 53:865–71. [PubMed: 12377295]
7. Marchi N, Granata T, Janigro D. Inflammatory pathways of seizure disorders. Trends Neurosci. 2014; 37:55–65. [PubMed: 24355813]
8. Loscher W, Potschka H. Drug resistance in brain diseases and the role of drug efflux transporters. Nat Rev Neurosci. 2005; 6:591–602. [PubMed: 16025095]
9. van Vliet EA, Aronica E, Gorter JA. Role of blood-brain barrier in temporal lobe epilepsy and pharmacoresistance. Neuroscience. 2014; 277:455–73. [PubMed: 25080160]
10. Dauchy S, Dutheil F, Weaver RJ, et al. ABC transporters, cytochromes P450 and their main transcription factors: expression at the human blood-brain barrier. JNeurochem. 2008; 107:1518–28. [PubMed: 19094056]
11. Dauchy S, Miller F, Couraud PO, et al. Expression and transcriptional regulation of ABC transporters and cytochromes P450 in hCMEC/D3 human cerebral microvascular endothelial cells. BiochemPharmacol. 2009; 77:897–909.
12. Ghersi-Egea JF, Leininger-Muller B, Cecchelli R, et al. Blood-brain interfaces: relevance to cerebral drug metabolism. ToxicolLett. 1995; 82–83:645–53.
13. Ghersi-Egea JF, Strazielle N. Choroid plexus transporters for drugs and other xenobiotics. JDrug Target. 2002; 10:353–7. [PubMed: 12164384]
14. Ghosh C, Gonzalez-Martinez J, Hossain M, et al. Pattern of P450 expression at the human blood-brain barrier: Roles of epileptic condition and laminar flow. Epilepsia. 2010
15. Ghosh C, Marchi N, Desai NK, et al. Cellular localization and functional significance of CYP3A4 in the human epileptic brain. Epilepsia. 2011; 52:562–71. [PubMed: 21294720]
16. Howard LA, Miksys S, Hoffmann E, et al. Brain CYP2E1 is induced by nicotine and ethanol in rat and is higher in smokers and alcoholics. Br J Pharmacol. 2003; 138:1376–86. [PubMed: 12711639]
17. Joshi M, Tyndale RF. Regional and cellular distribution of CYP2E1 in monkey brain and its induction by chronic nicotine. Neuropharmacology. 2006; 50:568–75. [PubMed: 16368115]
18. Mann A, Miksys SL, Gaedigk A, et al. The neuroprotective enzyme CYP2D6 increases in the brain with age and is lower in Parkinson's disease patients. Neurobiol Aging. 2012; 33:2160–71. [PubMed: 21958961]
19. Pardini C, Vaglini F, Viaggi C, et al. Role of CYP2E1 in the mouse model of MPTP toxicity. Parkinsonism Relat Disord. 2008; 14(Suppl 2):S119–23. [PubMed: 18583171]
20. Tindberg N, Baldwin HA, Cross AJ, et al. Induction of cytochrome P450 2E1 expression in rat and gerbil astrocytes by inflammatory factors and ischemic injury. Mol Pharmacol. 1996; 50:1065–72. [PubMed: 8913336]

21. Ferguson CS, Tyndale RF. Cytochrome P450 enzymes in the brain: emerging evidence of biological significance. Trends Pharmacol Sci. 2011; 32:708–14. [PubMed: 21975165]
22. Levy RH. Cytochrome P450 isozymes and antiepileptic drug interactions. Epilepsia. 1995; 36(Suppl 5):S8–13.
23. Kakizaki S, Takizawa D, Tojima H, et al. Nuclear receptors CAR and PXR; therapeutic targets for cholestatic liver disease. Front Biosci (Landmark Ed). 2011; 16:2988–3005. [PubMed: 21622216]
24. Wei P, Zhang J, Dowhan DH, et al. Specific and overlapping functions of the nuclear hormone receptors CAR and PXR in xenobiotic response. Pharmacogenomics J. 2002; 2:117–26. [PubMed: 12049174]
25. Wei P, Zhang J, Egan-Hafley M, et al. The nuclear receptor CAR mediates specific xenobiotic induction of drug metabolism. Nature. 2000; 407:920–3. [PubMed: 11057673]
26. Pascussi JM, Gerbal-Chaloin S, Drocourt L, et al. The expression of CYP2B6, CYP2C9 and CYP3A4 genes: a tangle of networks of nuclear and steroid receptors. Biochim Biophys Acta. 2003; 1619:243–53. [PubMed: 12573484]
27. Tolson AH, Wang H. Regulation of drug-metabolizing enzymes by xenobiotic receptors: PXR and CAR. Adv Drug Deliv Rev. 2010; 62:1238–49. [PubMed: 20727377]
28. Duveau V, Pouyatos B, Bressand K, et al. Differential Effects of Antiepileptic Drugs on Focal Seizures in the Intrahippocampal Kainate Mouse Model of Mesial Temporal Lobe Epilepsy. CNS Neurosci Ther. 2016; 22:497–506. [PubMed: 26899987]
29. Heinrich C, Lahteinen S, Suzuki F, et al. Increase in BDNF-mediated TrkB signaling promotes epileptogenesis in a mouse model of mesial temporal lobe epilepsy. Neurobiol Dis. 2011; 42:35–47. [PubMed: 21220014]
30. Jefferys J, Steinhauser C, Bedner P. Chemically-induced TLE models: Topical application. J Neurosci Methods. 2016; 260:53–61. [PubMed: 25960204]
31. Riban V, Bouilleret V, Pham-Le BT, et al. Evolution of hippocampal epileptic activity during the development of hippocampal sclerosis in a mouse model of temporal lobe epilepsy. Neuroscience. 2002; 112:101–11. [PubMed: 12044475]
32. Kolodkin A, Sahin N, Phillips A, et al. Optimization of stress response through the nuclear receptor-mediated cortisol signalling network. Nat Commun. 2013; 4:1792. [PubMed: 23653204]
33. Abbott RJ, Browning MC, Davidson DL. Serum prolactin and cortisol concentrations after grand mal seizures. J Neurol Neurosurg Psychiatry. 1980; 43:163–7. [PubMed: 6766989]
34. Stavropoulos I, Pervanidou P, Gnardellis C, et al. Increased hair cortisol and antecedent somatic complaints in children with a first epileptic seizure. Epilepsy Behav. 2017; 68:146–52. [PubMed: 28189919]
35. van Campen JS, Hompe EL, Jansen FE, et al. Cortisol fluctuations relate to interictal epileptiform discharges in stress sensitive epilepsy. Brain. 2016; 139:1673–9. [PubMed: 27036410]
36. Bauer B, Yang XD, Hartz AMS, et al. In vivo activation of human pregnane X receptor tightens the blood-brain barrier to methadone through P-glycoprotein up-regulation. Molecular Pharmacology. 2006; 70:1212–9. English. [PubMed: 16837625]
37. Woodland C, Huang TT, Gryz E, et al. Expression, activity and regulation of CYP3A in human and rodent brain. Drug Metab Rev. 2008; 40:149–68. [PubMed: 18259987]
38. Frye CA, Koonce CJ, Walf AA. Pregnane xenobiotic receptors and membrane progestin receptors: role in neurosteroid-mediated motivated behaviours. J Neuroendocrinol. 2013; 25:1002–11. [PubMed: 24028379]
39. Frye CA, Koonce CJ, Walf AA. Involvement of pregnane xenobiotic receptor in mating-induced allopregnanolone formation in the midbrain and hippocampus and brain-derived neurotrophic factor in the hippocampus among female rats. Psychopharmacology (Berl). 2014; 231:3375–90. [PubMed: 24781516]
40. Khandaker GM, Cousins L, Deakin J, et al. Inflammation and immunity in schizophrenia: implications for pathophysiology and treatment. Lancet Psychiatry. 2015; 2:258–70. [PubMed: 26359903]
41. Krahl SE, Clark KB. Vagus nerve stimulation for epilepsy: A review of central mechanisms. Surg Neurol Int. 2012; 3:S255–9. [PubMed: 23230530]

Key Points

1. The expression of specific cytochrome drug metabolic enzymes is increased in the liver and hippocampi during spontaneous recurrent seizures in mice.
2. GFAP immunoreactivity in the hippocampus positively correlates with Cyp over-expression during seizures
3. Hepatic and brain Cyp expression changes could impact drug biotransformation in the periphery or in the CNS during pathophysiology.

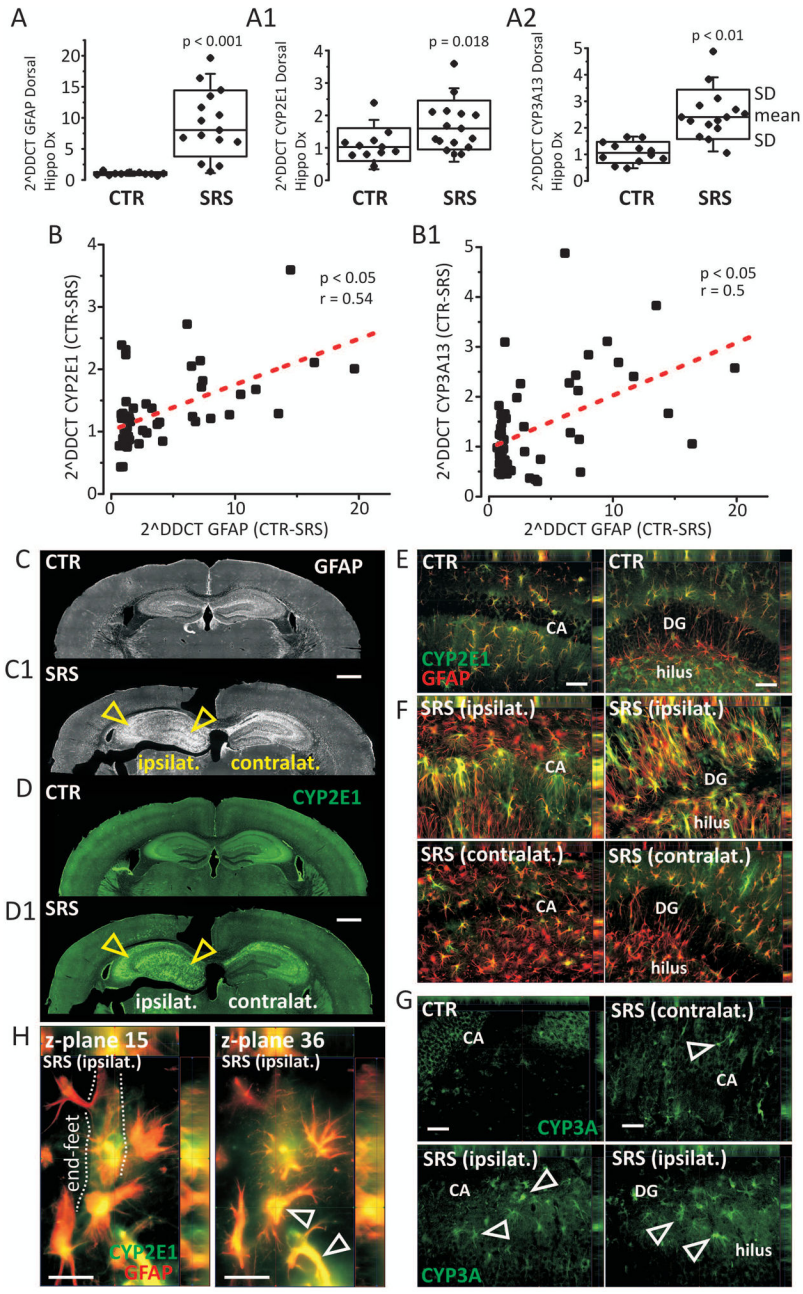

Figure 1. Cyp hippocampal over-expression during SRS and GFAP immunoreactivity

A–A2) RT-qPCR results showing a >10 fold increase in GFAP transcripts (ipsilateral) concomitant to Cyp2E1 and Cyp3a13 upregulation during SRS. The latter changes were less prominent or non-significant in the contralateral hemisphere (see Supplemental Figure 1A–A2). n = 4–5 mice/condition. Data are shown as box plot with individual values (mean ± SD). The non-parametric Mann-Whitney test was used, $p<0.05$. **B–B1)** Linear correlation between GFAP and Cyp expression as determined by RT-qPCR. **C–C1)** Typical pattern of GFAP immunoreactivity in the hippocampi at SRS. **D–D1)** Montage of Cyp2e1 immunoreactivity in control and SRS mice. **E–F)** Ipsilateral and contralateral Cyp2e1

expression co-localizes with GFAP immunoreactivity, the latter abundant in the ipsilateral side at SRS (CA and dentate gyrus, DG). **G)** Similar considerations applied to Cyp3A expression. **H)** Example of Z-stack planes showing Cyp-GFAP co-localization at the perivascular interface. Scale bars: 1 mm and 50 μm.

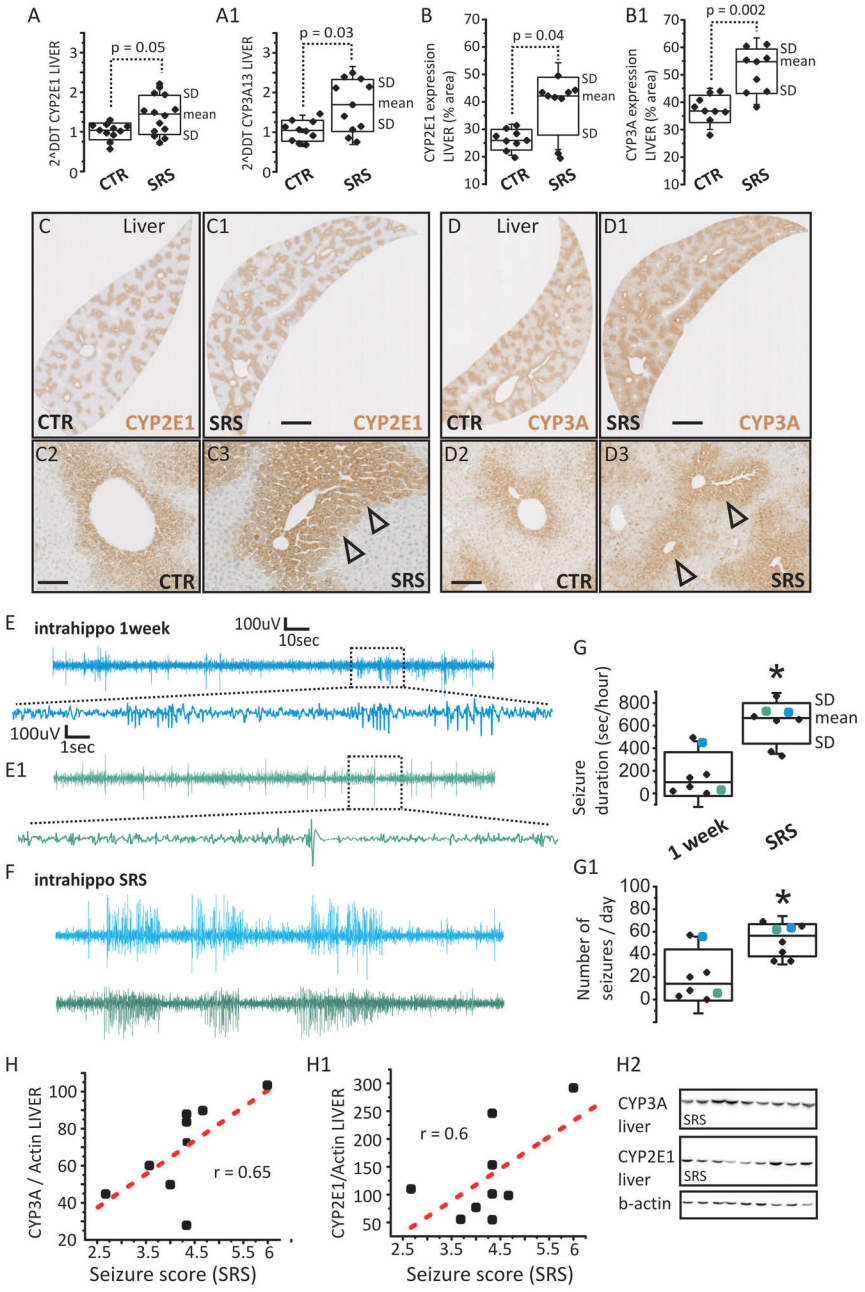

Figure 2. Increased hepatic Cyp expression during SRS

A–A1) RT-qPCR transcripts of Cyp were upregulated at SRS. **B–B1)** Cyp quantification expressed as % immunoreactivity area. n = 4–5 mice/condition (duplicate or triplicate). Data are shown as box plot with individual values (mean ± SD). The non-parametric Mann-Whitney test was used, $p<0.05$. **C–D)** Examples of Cyp2e1 and Cyp3a staining in liver samples obtained from control and SRS mice. Note the increased signals at SRS (*arrowheads*). Scale bars 1 mm and 50 μm. **E–E1)** Examples of intra-hippocampal EEG traces relative to low (green) and high (blue) seizing mice as detected 1 week after i.h. KA. **F)** At SRS mice displayed an overall increased seizure frequency and severity. **G–G1)**

Quantification of seizure duration and number of seizures in the cohort used. Data are shown as box plot with individual values (mean ± SD). Parametric t-test was used in D-D1, $p<0.05$. **H–H2)** Cyp hepatic protein levels at SRS positively correlates with EEG seizure scores (n = 9 mice).

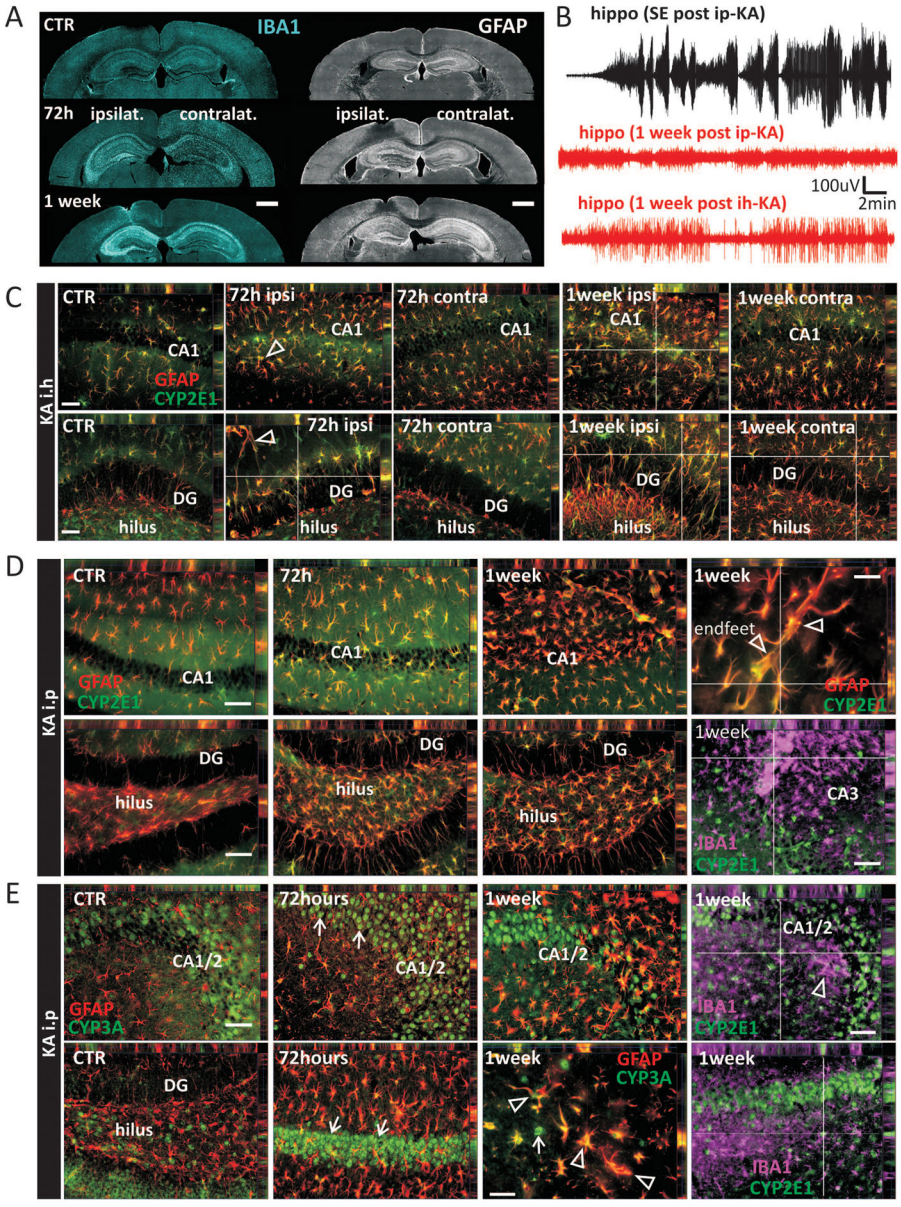

Figure 3. Patterns of Cyp hippocampal expression post-SE

A) Typical patterns of IBA and GFAP immunoreactivity in the hippocampi up to 1 week post-SE. **B)** Examples of intra-hippocampal EEG traces recorded after i.h. or i.p. KA (SE and 1 week post-SE). **C)** SE (i.h. injection) is sufficient to trigger Cyp increased (CA and dentate gyrus, DG). Ipsilateral changes were more robust as compared to contralateral (see also Figure 3). **D–E)** Patterns of Cyp2e1 and Cyp3a changes post-SE were confirmed using i.p. KA-injected mice. Note that Cyp co-localized with GFAP and not with IBA1+ activated microglial cells (*arrowheads*, CA and DG). Scale bars 1 mm and 50 μm. See also Table 1 for RT-qPCR Cyp transcript levels.

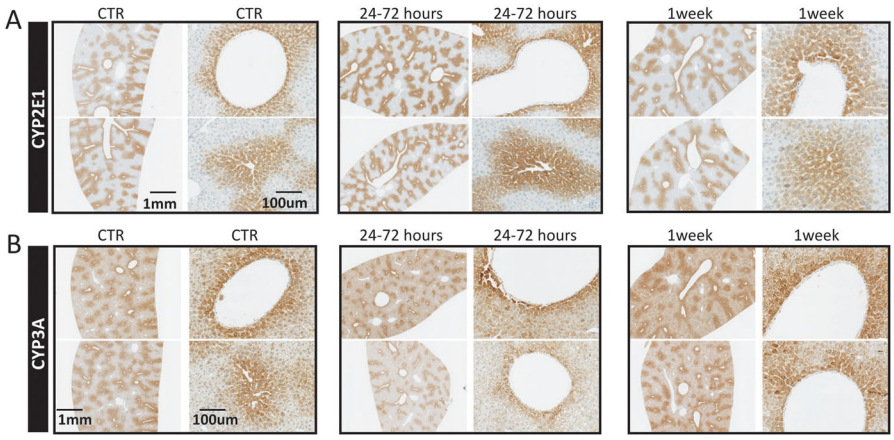

Figure 4. Patterns of Cyp hepatic expression post-SE

A–B) Cyp2e1 expression increased while Cyp3a expression transiently decreased 24–72 hours post-SE, returning to control levels 1 week after. See also Table 1 and Supplemental figure 1D.

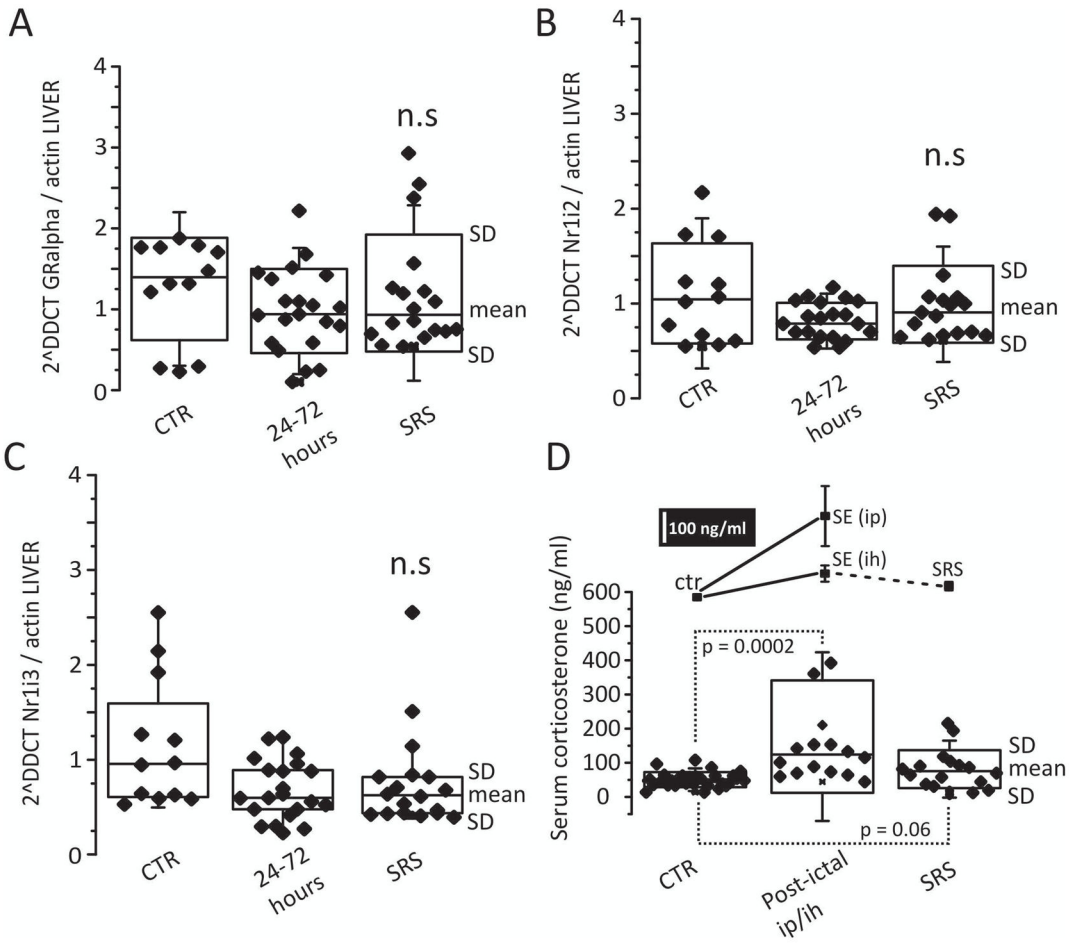

Figure 5. Nuclear receptors expression and serum corticosterone levels

A–C) Hepatic transcripts of selected nuclear receptors, known to respond to corticosterone (GR) and controlling Cyp levels (GR-NR1i) were stably expressed in SRS mice. **D)** Mean baseline corticosterone levels was 50.6 ± 22 ng/ml (SD), an accepted physiological values reported for *non*-stressed C57BL/6j male mice. Increased corticosterone serum levels were measured post-SE, induced either by i.p. or i.h. KA. Although variability existed, corticosterone levels were generally elevated in SRS mice as compared to control. n > 10 mice/condition in D, n = 4–5 mice/condition in A–C. Data are shown as box plot with individual values (mean ± SD). Non-parametric Mann-Whitney was used, $p<0.05$.

Table 1

Summary of RT-qPCR results obtained from liver and hippocampal samples in the two KA models

Data sets refer to i) control, 24–72h and 1 week post-SE, a time-frame common to the i.h. and i.p. KA models;ii) chronic experiencing SRS, specific to the i.h. KA model.

INTRA-HIPPOCAMPAL KA INJECTION							
Organ / Area	**Conditions (n = mice)**	**CYP2E1**	**CYP3A13**	**PXR (Nr1i2)**	**CAR (Nr1i3)**	**GR α**	**GFAP**
Liver	Control (n = 4)	1.009 ± 0.06	1.035 ± 0.08	1.107 ± 0.15	1.033 ± 0.08	1.251 ± 0.18	2.257 ± 0.66
	24h–72h (n = 7)	0.681 ** ± 0.07	1.075 ± 0.10	0.815 ± 0.04	1.354 ± 0.15	0.978 ± 0.11	0.682 * ± 0.16
	1 week (n = 4)	0.896 ± 0.15	1.315 ± 0.20	1.175 ± 0.19	1.034 ± 0.16	1.248 ± 0.23	0.559 ± 0.14
	Chronic (SRS; n = 6)	1.660 * ± 0.26	1.958 * ± 0.40	1.267 ± 0.29	1.567 ± 0.28	1.201 ± 0.17	1.412 ± 0.37
Hippocampi (Right)	Control (n = 4)	1.100 ± 0.15	1.074 ± 0.11	1.118 ± 0.16	1.023 ± 0.06	1.0485 ± 0.08	1.025 ± 0.07
	24h–72h (n = 9)	0.777 ± 0.11	0.772 * ± 0.12	0.607 ǂ ± 0.08	0.481 ǂ ± 0.04	0.569 ǂ ± 0.04	7.219 ǂ ± 0.66
	1 week (n = 3)	0.504 ** ± 0.09	1.575 * ± 0.19	1.031 ǂ ± 0.13	0.588 ǂ ± 0.05	0.797 * ± 0.08	8.635 ǂ ± 1.88
	Chronic (SRS; n = 5)	1.705 * ± 0.19	2.508 ǂ ± 0.24	1.143 ± 0.18	0.976 ± 0.06	1.175 ± 0.07	9.101 ǂ ± 1.37
Hippocampi (Left)	Control (n = 4)	1.141 ± 0.18	1.156 ± 0.24	1.191 ± 0.23	1.017 ± 0.06	1.027 ± 0.07	1.014 ± 0.05
	24h–72h (n = 8)	0.659 ** ± 0.08	0.395 ǂ ± 0.05	0.838 ± 0.08	0.690 ** ± 0.06	0.543 ǂ ± 0.03	6.985 ǂ ± 0.56
	1 week (n = 4)	0.624 * ± 0.11	0.906 ± 0.13	1.006 ± 0.13	0.671 ǂ ± 0.05	0.804 ** ± 0.05	8.427 ǂ ± 1.67
	Chronic (SRS; n = 5)	1.212 ± 0.08	0.689 ± 0.09	0.666 ± 0.07	0.899 ± 0.04	0.923 ± 0.08	3.377 ǂ ± 0.56
INTRA-PERITONEAL KA INJECTION							
Organ / Area	**Conditions (n = mice)**	**CYP2E1**	**CYP3A13**	**PXR (Nr1i2)**	**CAR (Nr1i3)**	**GR α**	**GFAP**
Liver	Control (n = 5)	1.826 ± 0.26	1.813 ± 0.12	1.157 ± 0.12	1.825 ± 0.13	1.065 ± 0.10	2.499 ± 1.17
	24h–72h (n = 10)	0.738 ǂ ±0.08	1.028 ǂ ± 0.11	0.575 ǂ ± 0.06	1.024 ǂ ± 0.10	0.876 * ± 0.12	1.906 ± 0.68
	1 week (n = 3)	2.185 ± 0.24	1.846 ± 0.35	0.946 ± 0.05	1.392 ± 0.16	0.879 ± 0.06	1.148 ± 0.29
Hippocampi	Control (n = 4)	1.141 ± 0.16	1.717 ± 0.45	1.282 ± 0.20	1.091 ± 0.12	1.044 ± 0.07	1.122 ± 0.10
	24h–72h (n = 9)	0.530 ǂ ± 0.06	0.711 ** ± 0.10	0.848 ± 0.09	0.699 ** ± 0.05	0.499 ǂ ± 0.03	9.481 ǂ ± 1.01
	1 week (n = 3)	0.858 ± 0.13	1.437 ± 0.21	1.224 ± 0.21	0.892 ± 0.11	0.703 ǂ ± 0.05	4.780 ǂ ± 0.55

* $p < 0.05$

** $p < 0.01$

$^{\ddagger}p < 0.001$